High-Frequency-Relaxation Measurements of Magnetic Specific Heats*

A. T. Skjeltorp and W. P. Wolf
Yale University, Becton Center, New Haven, Connecticut 06520
(Received 13 October 1972)

The recent development of cryogenic tunnel-diode oscillators has been used to improve and extend the high-frequency-relaxation (HFR) method for measuring the magnetic specific heat C_M. The method, originally due to Casimir and du Pré, uses purely magnetic measurements to determine C_M directly, without the usual correction for the generally much larger lattice contribution to the total heat capacity, and it thus allows accurate estimates of C_M over wide ranges of temperature. At temperatures that are high compared with the onset of magnetic ordering, C_M can be fitted to a series expansion of the form $C_M/R = C_2/T^2 + C_3/T^3 + \cdots$, where $R = Nk_B$ and N is the number of magnetic spins, and in suitable cases this can be related to microscopic spin-spin interaction parameters. Additional information can also be obtained from the field dependence of C_M, which can be related to the temperature dependence of the isothermal susceptibility. The central experimental requirement for this method is an accurate determination of the field and temperature dependence of the differential susceptibility in the MHz frequency range, and a fairly detailed discussion of a suitable system is given. Examples of materials for which this technique has been used succesfully include rare-earth halides, hydroxides, and garnets, but many other materials should satisfy the conditions under which this method can be applied. A review of these conditions is given and the criteria for choosing suitable measuring fields, frequencies, and temperatures are summarized.

I. INTRODUCTION

One of the most important quantities characterizing a magnetic system and its microscopic interactions is the magnetic specific heat C_M.[1] In particular, for a paramagnetic system at temperatures much higher than the ordering temperature, the magnetic specific heat can often be expressed as a simple series expansion in $1/T$,[2-4]

$$C_M/R = C_2/T^2 + C_3/T^3 + \cdots , \quad (1)$$

whose coefficients[5] C_2, C_3, ... can be related directly to the traces of different powers of the interaction Hamiltonian describing the system. An analysis of such an expansion can give useful information about the microscopic spin-spin interactions, and in suitable cases it may be possible to combine the specific heat results with susceptibility data to obtain a rather complete description of the various near neighbor exchange interactions. Examples of such analyses are given elsewhere.[6,7]

To obtain reliable experimental estimates of the coefficients C_2, C_3, ..., one requires accurate measurements of C_M over a wide range of temperatures. This is difficult with the usual calorimetric methods since they do not measure C_M directly, but instead measure the *total* specific heat, from which an estimated lattice contribution C_L must be subtracted to obtain C_M. Since C_L is generally much larger than C_M, even a small uncertainty in either the total or C_L can result in a considerable error in C_M. This error becomes larger as T increases since C_M falls off (roughly as $1/T^2$) while C_L increases (roughly as T^3). Thus C_M is most difficult to determine in just those regions in which Eq. (1) should be most applicable.

In this paper we shall review a powerful but strangely neglected technique which avoids the problem of the lattice contribution and determines C_M directly in terms of purely magnetic measurements. The basic method was first proposed by Casimir and du Pré[8] (CdP) in 1938 and was used extensively for a number of years, mainly by Gorter and his co-workers.[9-13] However, with the electronic techniques available at that time use of the method was difficult and not very precise, and apart from some very-low-temperature applications[14,15] it has lain practically forgotten during the past twenty or so years. However, the recent development of the tunnel-diode oscillators for use at low temperatures[16-22] coupled with the convenience and accuracy of electronic frequency counters and the stability of superconducting magnets, has completely changed the experimental situation, and the method should now prove useful for studying a wide class of magnetic materials.

As we shall see, the technique in its present form is most suitable for materials which order at 10–20 K or below, but it may be possible to extend the range in some special cases. Results already obtained indicate[6,23] that quite accurate measurements of C_M (± 2%) can be obtained at temperatures as high as 70 K where lattice contributions are many orders of magnitude larger than C_M, so that standard calorimetric estimates of C_M would be completely impossible.

At the same time, the method suffers from some intrinsic limitations which make it applicable only under certain conditions; we shall discuss these conditions in Sec. III. Specifically, we shall try

to define a set of criteria which will indicate whether a particular system is suitable for study by this method and what additional information may be required before accurate measurements of C_M can be made.

The experimental technique and recent developments in the apparatus are discussed in Sec. IV, and the analysis of the data is reviewed in Sec. V. Section VI contains a summary of various results which have been obtained so far and a discussion of the experimental errors, and the Sec. VII gives a brief evaluation of the future potential of the method.

II. BASIS OF METHOD

A. CdP Theory

The differential susceptibility of a paramagnetic system in a dc field H parallel to the measuring field generally depends on both the measuring frequency f and the strength of the dc field, and it has both in-phase and out-of-phase components

$$\chi(H, f) = \chi'(H, f) - i\chi''(H, f) \ . \tag{2}$$

The behavior is simplified under two conditions, first recognized by CdP,[8] which may be expressed as

$$1/\tau_{SL} \ll 2\pi f \ , \tag{3}$$

$$1/\tau_{SS} \gg 2\pi f \ , \tag{4}$$

where τ_{SL} and τ_{SS} are, respectively, the spin-lattice and spin-spin relaxation times.[24] Under these conditions the susceptibility becomes independent of frequency, the out-of-phase component vanishes and the in-phase component becomes equal to the thermodynamically defined adiabatic susceptibility $\chi'(H) \equiv \chi_S(H)$. This is related to the corresponding isothermal susceptibility, $\chi_T(H) = (\partial M/\partial H)_T$, by the thermodynamic relation

$$\chi_S(H) = \chi_T(H)(C_M/C_H) \ , \tag{5}$$

where C_H is the specific heat in constant field. Using the thermodynamic relationship

$$C_M = C_H - \frac{T(\partial M/\partial T)_H^2}{\chi_T(H)} \ , \tag{6}$$

one can eliminate C_H and obtain an expression for C_M,

$$C_M(H, T) = \left(\frac{T(\partial M/\partial T)_H^2}{\chi_T(H)}\right)\left(\frac{\chi'(0)}{\chi'(H)}\,\frac{\chi_T(H)}{\chi_T(0)} - 1\right)^{-1} \ , \tag{7}$$

where we have used the fact that $\chi'(0) = \chi_S(0) = \chi_T(0)$ to introduce an extra factor $\chi'(0)/\chi_T(0) \equiv 1$ which will simplify the subsequent analysis.

From this expression we see how $C_M(H, T)$ can be found directly from measurements of the relative field dependence of the differential susceptibility measured under adiabatic conditions, provided that one also knows the static magnetization $M(H, T)$ in the field and temperature region in question. Since M must be known well enough to permit estimates of the various derivatives, this may be a nontrivial condition, but in most cases a sufficiently accurate approximation for M can be derived. We shall discuss this point further in Sec. VC and the Appendix.

It should be pointed out that the factor $\chi_T(H)/\chi_T(0)$ in Eq. (7) tends to 1 for small H, and it is therefore often neglected.[9-12] However, inasmuch as $\chi'(0)/\chi'(H)$ also tends to 1 as $H \to 0$, this approximation may introduce a sizable error and careful examination of the two low-field limits is required. We shall consider some specific cases of this factor in the Appendix.

B. Field Dependence of Magnetic Specific Heat

The magnetic specific heat determined in the presence of a dc magnetic field H will generally be a function of H. To extract the quantities most directly related to the intrinsic interactions, it is necessary to analyze this field dependence, and in particular to extract the specific heat in zero field $C_M(0, T)$.

From the definition

$$C_M = T\left(\frac{\partial S}{\partial T}\right)_M \ , \tag{8}$$

it follows that

$$\left(\frac{\partial C_M}{\partial M}\right)_T = T\,\frac{\partial}{\partial T}\left(\frac{\partial S}{\partial M}\right)_M \ , \tag{9}$$

and using the Maxwell relation

$$\left(\frac{\partial S}{\partial M}\right)_T = -\left(\frac{\partial H}{\partial T}\right)_M \ , \tag{10}$$

we find

$$\left(\frac{\partial C_M}{\partial M}\right)_T = -T\left(\frac{\partial^2 H}{\partial T^2}\right)_M \ . \tag{11}$$

Integrating, we obtain

$$C_M(0, T) = C_M(H, T) + \int_0^M \left(\frac{\partial^2 H}{\partial T^2}\right)_M dM \ . \tag{12}$$

If, as we already suppose, we know $M(H, T)$, the last term in this expression can readily be evaluated.

There are two common cases in which this correction becomes trivial. If M in the region of H and T of interest is given to a sufficient approximation by either

$$M = \lambda H/(T - \theta) \tag{13}$$

or by any function of H/T,

$$M = f(H/T) \ , \tag{14}$$

we see immediately that $(\partial^2 H/\partial T^2)_M$ vanishes, so that C_M becomes independent of H. Indeed it was for this reason CdP first expressed their analysis in terms of C_M rather than C_H, since this quantity would depend on H, even in the simplest cases.

The vanishing of the field dependence of C_M in these special cases has in the past led to the mistaken assumption that the CdP method measures in effect the zero-field magnetic specific heat, which is directly related to the spin-spin interactions. However, from Eq. (12) we now see that this is only an approximation and that some form of extrapolation to zero field will generally be necessary. We shall discuss this point further in Secs. V D and V E.

III. APPLICATION TO SPECIAL SYSTEMS

It can be seen from the discussion in Sec. II that the relaxation method for measuring specific heats is only applicable under certain conditions. These conditions are related directly or indirectly to other properties, and for any particular system it is therefore necessary to establish whether the method can be used at all and if so, over what ranges of frequency, temperature and field useful measurements can be made.

A. Measuring Frequency

Appropriate frequency ranges are determined by the two inequalities given in Eqs. (3) and (4), and to determine whether some particular frequency will be satisfactory we must estimate τ_{SL} and τ_{SS}. However, we may immediately note that since τ_{SL} is usually a rapidly decreasing function with increasing temperature[25,26] while τ_{SS} is essentially temperature independent,[26-28] the highest frequency consistent with Eq. (4) will generally allow measurements over the widest temperature range.

To estimate τ_{SL} in any particular case we can follow one of two approaches. If the system is reasonably well understood from the point of view of its crystal field and lattice interactions, a rough theoretical estimate of the various mechanisms contributing to τ_{SL}^{-1} can be made[25] and this may often be adequate for determining the temperature limit below which a given frequency will satisfy Eq. (3).

Alternately, one can proceed empirically measuring χ' in a fixed field as a function of temperature, starting at some low temperature where the inequality is certainly met, and increasing the temperature until there is evidence that the spins and the lattice are no longer isolated from one another. This change manifests itself by a marked increase in the apparent adiabatic susceptibility, corresponding to the fact that C_M is replaced by $C_M + C_L$ as soon as the spins are able to stay in thermal equilibrium with the lattice. Since C_L is generally much larger than C_M, this results in a marked reduction of $\chi'(0)/\chi'(H)$ which can readily be observed.

The spin-spin relaxation time is more difficult to estimate, but fortunately it is usually so short that it rarely provides an effective upper limit to the frequencies which can be used. In rare cases such as those of highly anisotropic systems in which spin-spin relaxation may be anomalously slow,[29] a check of Eq. (4) can be made by comparing the absolute value of the zero-field susceptibility measured at high frequency with low-frequency measurements, or with theoretical estimates of the susceptibility. In the event that τ_{SS}^{-1} is not much larger than $2\pi f$, there will be a significant reduction in the observed high-frequency susceptibility, and indeed if $2\pi f$ happens to be much larger than τ_{SS}^{-1} no magnetic susceptibility will be measured at all.

A second check for the adequacy of Eq. (4) is provided by the final analysis for C_M, since τ_{SS} is generally a rapidly varying function of H (Ref. 27), and unless $\tau_{SS}^{-1} \gg 2\pi f$ throughout, this will manifest itself as an anomalous field dependence of $\chi'(0)/\chi'(H)$.

The upper frequency limit is usually set by experimental considerations, and with our present apparatus the limit turned out to be about 100 MHz. In many cases considerably lower frequencies may be quite adequate to satisfy the lower CdP limit [Eq. (3)], and in practice we have generally used various frequencies between 1 and 5 MHz. Of course much lower frequencies can also be used,[9] but the range of temperatures over which the adiabatic conditions apply then becomes much smaller.

A final check of the relaxation conditions should be made in all cases by comparing specific-heat values determined at two different frequencies, using if possible frequencies differing by a factor of 2 or more. This procedure also has the advantage of verifying that adequate dielectric corrections have been made (see Sec. V B).

B. Temperature Range

The temperature ranges over which useful specific-heat measurements can be made is determined by two quite unrelated conditions. The first is linked directly to the particular frequency which has been chosen, as discussed above. In practice it turns out that a measuring frequency of, say, 50 MHz sets a limit in the range of 10–20 K for systems with strong orbit-lattice coupling, and a factor of 10 higher for systems which have no orbital angular momentum.[9-13]

The second condition reflects the fact that a detailed final analysis can only be made if both the specific heat and magnetization can be represented

in terms of simple expressions which can be characterized by only a few parameters. In particular we require a fairly accurate approximation for $M(H, T)$, and this is generally available only for $T \gg T_c$, where T_c is the ordering temperature. Under this condition the expansion of C_M [given in Eq. (1)] is generally also valid[30] and the final result can be analyzed very simply.

For temperatures close to T_c accurate analytic expressions for $M(H, T)$ are generally not available, but in some cases it may be possible to extract the various derivatives required in Eq. (7) from empirical magnetostatic data. It should then be possible to determine C_M also in this range. However, in most cases the condition $T \sim 2T_c$ is probably a more realistic statement of the lower-temperature limit.

C. Magnetic Field Range

The magnetic field required to produce a significant change in χ' depends on the size of the specific heat and the magnetic properties, as indicated by Eq. (7). A rough estimate of the field required to reduce χ' to half its zero-field value can be obtained by approximating $M(H, T)$ by Curie's law, $\lambda H/T$,[31] and this gives

$$H' = (C_M T^2/\lambda)^{1/2} \quad . \tag{15}$$

In some cases a field much smaller than H' can give a measurable change in χ', and with the present apparatus we have been able to use fields as small as $\frac{1}{5}H'$ and still measure the change in χ' to better than 3%.

There are several reasons for using fields as small as possible. First it simplifies the problem of finding an adequate approximation for $M(H, T)$, as we shall discuss in more detail in Secs. III D and V C. Secondly, it reduces the correction which must be made to find $C_M(0, T)$ from the measured $C_M(H, T)$ and if this can in fact be negligibly small, a considerable simplification in the analysis results. We shall discuss this further in Sec. V D. Thirdly, the ability to use relatively smaller fields extends the range of materials which can be studied by this method.

Some typical values of H' are shown in Table I, which summarizes the materials which have been studied so far.[6,7,23,32-38] One can see that while there is a very rough correlation between the values of H' and the ordering temperatures, there are also some large deviations which make T_c a poor measure of the actual H' [cf. the values for $Gd(OH)_3$ and $Tb(OH)_3$]. In practice, the maximum field available in any given apparatus cannot easily be changed, and a material with a relatively large specific heat can only be studied if correspondingly smaller changes in χ' can be measured with sufficient accuracy.

All these considerations point to the desirability of designing an apparatus as stable and as sensitive as possible and it is in this respect that the new tunnel-diode oscillators have resulted in a significant advance over earlier vacuum-tube oscillators. We shall discuss the design and performance of our particular tunnel-diode oscillators in Sec. IV B.

D. Magnetostatic Approximations

As we have seen in Eq. (7), it is necessary to estimate values of the magnetostatic quantities $(\partial M/\partial T)_H$, $(\partial M/\partial H)_T = \chi_T(H)$, and $(\partial M/\partial H)_{T,H=0} = \chi_T(0)$ before one can evaluate C_M from a measurement of $\chi'(0)/\chi'(H)$. There is of course no exact expression for M as a function of H and T from which these derivatives can be calculated in general, and for each case an appropriate approxima-

TABLE I. Magnetic systems investigated by HFR method.

Material	T_c (K)	Method[a]	Frequency (MHz)	Temp. (K)	H'[b] (kG)	$M(H, T)$ app.[c]	Ref.
$CeCl_3$	0.1	FD	8.5–22	1.2–4.2	0.95	*D*	32
$CeBr_3$	≤0.1	FD	8.5–22	1.2–4.2	1.3–1.4	*D*	33
$GdCl_3$	2.2	FD	12–37	20.7, 77	5.8	*D*	23
$Gd(OH)_3$	0.9	BD	4.5	5–70	5.7–6.9	*D*	6
$Tb(OH)_3$	3.7	BD	2–4	5–16	3–2	*D*	7, 34
DAG[d]	2.5	BD	0.8–2.1	5–12	3.9–4.3	e	35
CES[f]	0.03	FD	10–55	1.1–4.2	2–20	g	36[h], 37[h]
NES[i]	<0.1	FD, BD	0.4–46	1.5–4.2	0.3	*A*	38[h]

[a]Refers to the type of tunnel diode oscillator, using either a forward-biased diode (FD) or backward-biased diode (BD).

[b]Effective field estimated from Eq. (15).

[c]Approximation for $M(H, T)$ denoted by the cases discussed in Appendix.

[d]Dysprosium aluminum garnet.

[e]Using a perturbation calculation exact in the field and correct to second order in the interactions (Ref. 35).

[f]Cerium ethyl sulfate.

[g]Magnetization estimated for the two lowest Ce^{3+} doublets.

[h]Includes also investigation of relaxation processes.

[i]Neodymium ethyl sulfate.

tion must be made. This may either be based on prior knowledge of the system (ESR, optical spectra, etc.) or an empirical study of its magnetostatic properties.

For both approaches it is generally convenient to expand the magnetization of a paramagnetic crystal in odd powers of H:

$$M=\sum_{n=0}^{\infty} a_{2n+1}H^{2n+1} \quad , \tag{16}$$

where the a's are functions of temperature and the interactions.[39] Differentiating and substituting in Eq. (7) we then obtain

$$C_M(H,T)=\frac{T\left[\sum_{n=0}^{\infty}(\partial a_{2n+1}/\partial T)_H H^{2n+1}\right]^2}{\sum_{n=0}^{\infty}(2n+1)\,a_{2n+1}H^n} \times\left(\frac{\chi'(0)}{\chi'(H)}\,\frac{\sum_{n=0}^{\infty}(2n+1)\,a_{2n+1}H^n}{a_1}-1\right)^{-1} . \tag{17}$$

To find $C_M(0,T)$ one must next invert the expression in Eq. (16) to obtain an expression for H in terms of M:

$$H=\sum_{n=0}^{\infty} b_{2n+1}M^{2n+1} \quad , \tag{18}$$

where

$$b_1=1/a_1 \quad ,$$
$$b_3=-a_3/a_1^4 \quad ,$$
$$b_5=3a_3/a_1^7-a_4/a_1^6 \quad ,$$
$$\vdots$$

and using this in Eq. (12) one then finds

$$C_M(0,T)=C_M(H,T)+T\sum_{n=0}^{\infty} d_{2n+2}M^{2n+2} \quad , \tag{19}$$

with

$$d_{2n+2}=\frac{1}{2n+2}\,\frac{\partial^2}{\partial T^2}\,(b_{2n+1}) \quad . \tag{20}$$

We shall consider a number of specific approximations for the a's in the Appendix and we shall relate some of these to specific systems in later sections. However, in considering any particular system, explicit attention must always be given to the field and temperature ranges in which measurements are to be made, and this often leads to a feedback control of the fields and temperatures which may in fact be used. As always, the problem is that the number of characteristic parameters which can be determined is quite limited, and only severely truncated expressions for M can generally be used. In practice this tends to restrict the whole method to relatively "high" temperatures and "low" fields, but with care these limitations can be partially overcome.

E. Anisotropy Effects

We have so far ignored possible anisotropy effects, and this is equivalent to considering only single crystals with fields applied along a principal axis. In other cases the discussion will be more complicated, and in particular the experimentally appealing case of a powder of anisotropic crystallites requires very careful treatment. Under most circumstances the individual crystallites have to be treated as separate thermodynamic systems and each grain will then have its own spin temperature and correspondingly its own adiabatic susceptibility. In principle, the different contributions can be averaged,[15] but in practice this procedure will be satisfactory only in special cases.

We must conclude, therefore, that an additional requirement for the application of the present method is that either the anisotropy is negligibly small as in the case of a cubic material, or that single crystals are available.

IV. EXPERIMENTAL METHOD

A. General Considerations

As we have seen, the central experimental problem is the measurement of the field dependence of the adiabatic susceptibility, and for the maximum temperature range this calls for a technique for measuring χ' in the MHz region. This can be done in various ways, but perhaps the simplest and most sensitive is to use a tunnel-diode oscillator operating inside the cryostat. The basic operation of this method has been described in some detail by Clover and Wolf,[21] who also give references to earlier work on related experiments. We shall therefore restrict ourselves here to a very brief outline of the technique and a discussion of recent developments.

Basically, the method consists of measuring the frequency change Δf when a sample is moved into the tank coil of a freely running oscillator. If the sample introduces no additional losses (as will be the case if $\chi''=0$ and there are no eddy currents) and the frequency change is small, then Δf will be the sum of two contributions

$$\Delta f=\Delta f_M+\Delta f_D \quad . \tag{21}$$

Here $\Delta f_M=2\pi F f\chi'$ is the magnetic shift which is directly proportional to the required susceptibility where F is the filling factor of the coil, and Δf_D is a dielectric shift which arises from the change in stray capacitance when the sample is moved relative to the oscillator.

The dielectric shift increases quite rapidly at higher frequencies[21] and it is therefore desirable to reduce it as much as possible by suitable design of the oscillator and sample holder. We shall discuss this problem in Sec. IV G, but we can al-

TABLE II. Typical components used in tunnel-diode oscillators.

Diode	Type oscillator coil Length (cm)	Diam (cm)	n[a]	L_s (μH)	C_s[b] (pF)	C_1[b] (pF)	C_2[b] (pF)	Frequency[c] f(MHz)
BD[d]	2.1[e]	1.2	110	80[f]	2500	470	20	0.4
BD	1.2[e]	1.2	60	40[f]	470–2000	100	20	1.6–0.7
BD	1.2[e]	0.7	40	7[f]	470	3000	20	2.6
BD	4.5[g]	0.2	500	14[f]	100–300	470	20	4.5–2
FD[h]	2.3[i]	1.2	14	1.3[j]	300–1500	1000	15	8.5–4
FD	1.5[i]	1.2	10	0.6[j]	10	390	15	18
FD	1.2[i]	1.2	6	0.12[j]	0	300	15	50
FD	1.0[i]	1.2	4	0.09[j]	10	100	0	100

[a]Number of turns.
[b]Low-loss (polystyrene) capacitors.
[c]Note that the components may differ from their nominal values, so that the calculated frequencies do not necessarily agree with the measured frequencies listed.
[d]BD = backward-biased tunnel diode BD-5.
[e]Hand-wound copper wire 30–34 AWG.
[f]Estimated $L_s(\mu H) \simeq 9.9\times10^{-3}\ (d^2/l)n^2$, where d = diam, l = length of coil (in cm), and n is the number of turns.
[g]Hand-wound copper wire 40 AWG.
[h]FD = forward-biased tunnel diode 1N3712.
[i]LRC Electronics metal-on-glass coils.
[j]Nominal L_s values.

ready note here that the residual correction for Δf_D will constitute the largest uncertainty in the determination of χ'. It is therefore most desirable to maximize the magnetic shift, and in practice this entails making a special oscillator coil for each sample so as to get the filling factor F as close to 1 as possible.

The large filling factor and dielectric correction generally tend to make Δf quite sensitive to sample position relative to the oscillator, and a rather reproducible sample transport is therefore required. We shall describe our particular mechanism in Sec. IV E, but we can note that since we really only require the *relative* field dependence of χ', i.e., $\chi'(0)/\chi'(H)$, we can obtain this by moving the sample only at the beginning and end of each field sweep (see Sec. IV C). However, this in turn requires a stable system with respect to temperature, field fluctuations, and oscillator frequency, and we therefore have to pay special attention to these factors in the design.

B. Oscillator Design

Tunnel-diode oscillators (TDO) have frequently been used for low-temperature applications. Originally the so-called back diodes (BD) were used as the active element primarily because of their low operating levels and consequently small power dissipation.[16,17] Subsequent applications have included low-temperature thermometry[18–20] and determination of magnetic transitions.[22] So-called forward-biased tunnel diodes (FD) can also be used for similar applications, since these offer a wider frequency range than the BD and it is also easier to build FD oscillators to operate over a large temperature range.[21] The potential disadvantage of FD is that it dissipates more power, but for many applications this is immaterial. Thus in our original apparatus for measuring high-frequency susceptibilities,[21] we chose to use a FD and were able to achieve frequencies between 1 and 100 MHz from helium temperatures up to room temperature. On the other hand, for some applications such a large range of temperatures and frequency is not necessary, and it then becomes possible to choose between the two kinds of diodes on the basis of stability of the corresponding oscillators. Such a comparison has shown that the original BD oscillators are in fact significantly more stable, and for all applications below 10 MHz we have therefore used only oscillators of this type. The BD oscillators also have the minor advantage that lower frequencies (~0.4 MHz) can be obtained more easily, but they have the disadvantage that they will oscillate only below about 200 K. However, for most of the specific-heat experiments which have been made so far this was immaterial and the better stability was overriding.

In Table II we give a list of typical combinations of circuit elements which have been used successfully for the BD and FD oscillators. The circuit diagram for our particular BD oscillator is shown in Fig. 1, and it can be seen that it is only slightly different from the circuit which was used previously.[21] The range of values shown for the various components reflects not only the different frequencies used, but also the widely different sizes of the oscillator coils made to conform to the different samples available. The smallest coils used were about 2 mm in diameter, and with these filling factors of the order of 0.01 could be obtained even with samples as small as 2 mg in mass.

Several practical precautions were followed in the construction of the oscillators. The oscillator

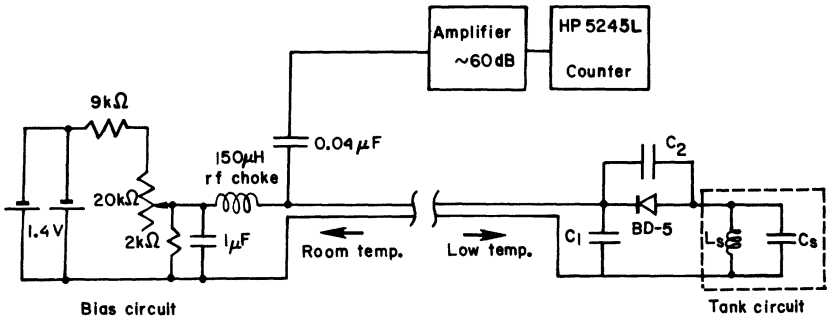

FIG. 1. Backward tunnel-diode oscillator used for susceptibility measurements.

circuit elements were mounted rigidly on a holder (Sec. IV F) using GE varnish No. 7031, and an eutectic Cd/Bi solder (nonsuperconducting down to $T = 0.8$ K) was used for all soldering. The dc leads from the bias circuit at room temperature to the oscillator were fixed at several points to the steel tube support for the low-temperature probe (Sec. IV F) so as to reduce microphonic noise. Because the frequency of a TDO is a function of the bias current, special care was also taken in the construction of the bias circuit. The batteries used for biasing were Duracell 1.4-V mercury cells which proved to have very stable voltage-versus-time characteristics. In addition, precision metal-film resistors were used in the bias circuit to ensure low voltage drift. The bias was adjusted in the beginning of an experiment and never changed thereafter.[40]

C. Frequency Stability and Sensitivity

The short-term stability (minutes) in the frequency f of the TDO using the BD was about $10^{-7}f$ and the long-term drift ($\frac{1}{2}$ h) about $10^{-6}f$. These figures were about a factor of 10 better than those which normally could be obtained using the FD. In order to measure frequencies to this accuracy it was convenient to use a Hewlett-Packard 5245L with 10-sec gate time to obtain a frequency resolution of 0.1 Hz.

In addition to the intrinsic stability of the oscillator there were also occasional larger frequency jumps, $\sim 10^{-5}f$, after the sample had been moved relative to the coil. The origin of these jumps could not be determined, but they could be eliminated almost completely in measurements of the field dependence of Δf using a field-sweep method. For the sample fixed in the coil, the field was increased stepwise and the frequency recorded after each increment of the field. Reducing the field through the same steps with the sample out of the coil, the frequency was again recorded and the frequency shift was found as the difference between the corresponding frequency readings. This technique also avoided uncertainties in the repositioning of the sample in the coil, as only relative measurements of Δf were needed. During the course of such a sweep, spurious frequency jumps ($\sim 10^{-5}f$ or less) were sometimes observed, presumably due to some mechanical disturbance in the cryostat. Such shifts could be detected quite readily by a routine check of one of the earlier frequency readings at the end of a field sweep; but usually the agreement was within $\pm 10^{-6}f$ and it seemed reasonable to assume that the intervening measurements would also be consistent to this accuracy.

It goes without saying that care was taken not to disturb any part of the apparatus (whether obviously connected to the TDO or not) while a field-sweep series of measurements was in progress, and indeed spurious frequency changes could occasionally be produced by such changes as turning large values on the apparatus, changing certain electrical contacts in other parts of the apparatus and operating noisy electrical equipment too close to the apparatus. Also, care was taken to allow the temperature of the oscillator return to equilibrium after each movement of the sample; especially one involving the replacement of the sample, which inevitably raised the temperature by a small amount (~0.1 K).

With care a limiting frequency stability $\sim 10^{-6}f$ could thus be achieved, and using this we can derive a rough estimate of the sensitivity of the best present set up for measuring C_M. If we require an accuracy of 1% in $\Delta f_M(0)/\Delta f_M(H)$ and we apply fields such that $\Delta f_M(0)/\Delta f_M(H) \sim 10$,[41] we find that we must have $2\pi F\chi'(0) \geq 10^{-3}$. Taking a typical filling factor $F \simeq 0.5$, this implies a susceptibility $\chi'(0) \simeq 0.003$ emu/cm^3. This may be compared, for example, with the susceptibility of a relatively dilute salt such as manganous ammonium sulfate which at 10 K is 0.002 emu/cm^3. It is thus evident that the present system is quite adequate for measuring typical paramagnetic salts over a reasonable range of temperatures. However, it is always desirable to improve the sensitivity and accuracy, and with this in view we have recently used a double oscillator which we shall describe in Sec. IV D.

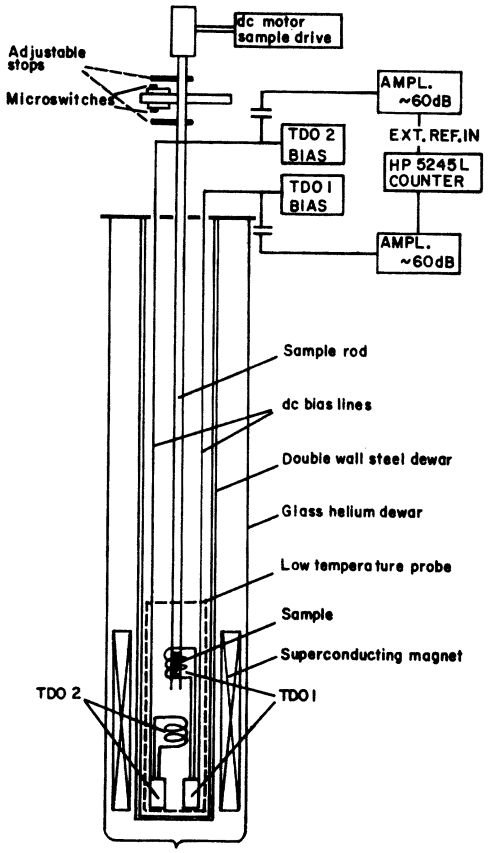

FIG. 2. Simplified diagram of the susceptibility apparatus and the electrical circuit.

D. Double Oscillators

Although the simple TDO described above proved to be quite stable under equilibrium conditions, it did have the undesirable characteristic of changing its frequency somewhat whenever either the field or the temperature were changed. The effects were generally small (typically 5–10 kHz for temperature variation between 4 and 50 K and 0.5–1 kHz for fields between 0 and 20 kOe) and in principle the frequency variation due to the background would have no effect on the measured frequency shifts Δf, as these were recorded with the sample in and out of the coil at the same field and temperatures. However, in practice, it would have been much more convenient if the frequency variations could be eliminated empirically as in this case possible small frequency drifts after resetting of field or temperature would be avoided. With this in mind, we constructed a double-oscillator system,[22] consisting of two TDO's made as similar as possible, one of them (TDO1) serving to measure Δf as in the previously described system, the other (TDO2) providing a reference frequency f_2 whose field and temperature dependence might be expected to mirror that of TDO1 in the absence of a sample. The ratio of the two frequencies f_1/f_2 should then be independent of both H and T and thus provide a much more stable base from which the effect of the sample might be determined. In practice the previously quoted frequency variations due to temperature and field variations could readily be reduced by a factor of 10–100 using this arrangement.

To monitor the frequency we found it convenient to use the HP 5245L counter operating in its external mode with TDO2 supplying the reference frequency f_2, so that the ratio f_1/f_2 could be read directly. With a 10-sec gate time this provided a resolution $\pm (f_1/f_2)\times 10^{-7}$ which corresponds to ± 0.1 Hz for a typical frequency $f_2 = 1$ MHz. This is the same resolution obtained using only one oscillator as described in Sec. IV C.

E. Sample Transport

As mentioned previously, it is not desirable to move the sample relative to the oscillator more often than necessary, since there is always a possibility of a spurious frequency shift whenever the apparatus is disturbed in any way. Nevertheless, it is generally necessary to move the sample some time during each field sweep, so that the frequency with the coil empty can be measured, and for this purpose a smoothly acting and reproducible sample transport is required. The mechanism used in our apparatus is shown schematically in Fig. 2, but many other forms could probably be used equally sucessfully.

The important features are a smooth sample motion over a distance of about 2 cm, reproducible to better than about 0.02 cm at the lower end of the travel. In our device the motion could be produced either manually or by means of a dc motor which was controlled using adjustable stops fastened to the sample rod hitting one microswitch when the sample was in the upper position and another when the sample was in the lower position. In practice we found the manual operation a little more reproducible. It is not clear whether this was due to deficiencies in the end-stop mechanism or to small electrical disturbances to the oscillator caused by operation of the motor. No serious attempt was made to improve the transport since this was not a limiting factor in our total system, but it is not hard to see how more sophisticated devices could be made.

The actual reproducibility in any particular case depended on the filling factor F and on the final position of the sample inside the coil, and care was always taken to find the effective center of the coil. For samples with a small filling factor the adjustment was less critical, but of course the frequency shift was then also less. The re-

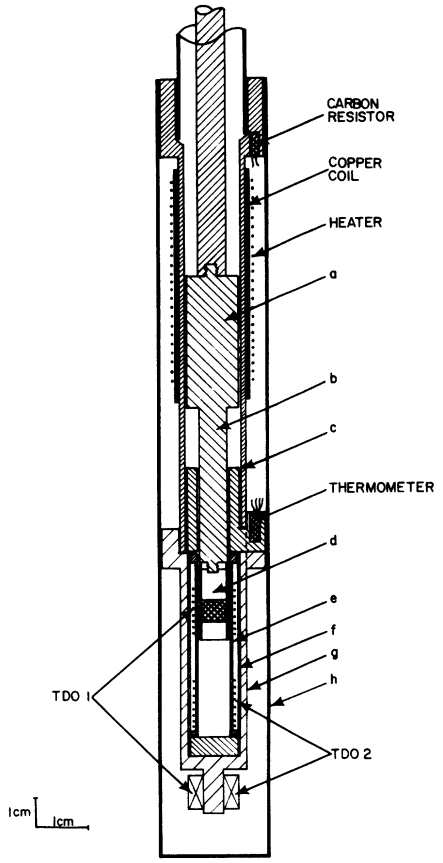

FIG. 3. Details of the low-temperature probe in Fig. 2. The letters refer to various components of the probe which are explained in the text.

placement reproducibility is thus best expressed as a percentage of the frequency shift, $\delta(\Delta f)/\Delta f$, and for our system this turned out to lie between about 10^{-3} and 5×10^{-2}. This gives a measure of the accuracy with which for example the temperature dependence of χ' could be measured, in contrast to the field dependence, which was limited primarily by the long term stability of the oscillator, as discussed in Sec. IV C.

F. Cryostat and Temperature Control

In the first version of our apparatus[21] the sample and oscillator were immersed directly in the appropriate cryogenic fluid (He, H_2, or N_2) and the temperature was controlled and measured by the vapor pressure. This arrangement was not satisfactory for several reasons. First, it allowed measurements only over three restricted temperature ranges; second, it made accurate temperature control difficult; and third, and most important, bubbles from the cryogenic fluid tended to disturb the oscillator.

To remove these difficulties, a variable-temperature cryostat was constructed and this is shown schematically in Fig. 2, together with experimental arrangement of the electrical circuits. In this system the sample was attached to a variable-temperature probe which was surrounded by helium gas at about 0.1–1 torr inside a double-wall steel Dewar and this in turn was immersed in liquid helium. By adjusting the residual gas pressure in the vacuum space of the Dewar, a variable heat leak from the sample could be produced and this could be balanced by means of an electrical heater on the probe.

Details of the probe are shown schematically in Fig. 3. The moving parts consisted of a long phenolic sample rod to which was attached a copper cylinder (a) with an extension piece (b) carrying the Teflon sample holder (d). The copper cylinder (a) was made to slide smoothly inside a fixed copper tube (c), the upper end of which carried the heater and the temperature sensors. The sample holder (d) could move in and out of a thin walled phenolic coil former (e) which carried the coils of both the main oscillator (TDO1) and the dummy oscillator (TDO2). The coil former was surrounded by a copper heat shield (f) which was thermally anchored to (c). The circuit elements of both TDO1 and TDO2 were mounted on phenolic holder (g) which fitted outside (f). The whole probe was enclosed in a copper tube (h).

Two sensors were used to control the temperature in the range from about 1.5–100 K. For temperatures below about 30 K an Allen Bradley $\frac{1}{10}$-W 100-Ω carbon resistor was used,[42] while above 30 K a coil of about 5000 turns of 44 gauge enameled copper wire wound noninductively on a 1-cm copper tube (c in Fig. 3) was used[43] (room temperature resistance about 1700 Ω). A standard ac bridge and feedback circuit were used to control the temperature in the usual way.[44]

Although both the sensors used were quite sensitive to temperature changes and also virtually free from significant magnetoresistive effects,[45] they were not entirely reproducible when cycled between room temperature and liquid helium. A separate semiconducting thermometer[46] was therefore used to measure the actual temperature and for this purpose a simple dc four-wire pontentiometer system was used.[47] Since the semiconductor showed the usual rather large magnetoresistance, all temperature measurements were made in zero field.

The estimated *accuracy* of the temperature measurements was about 5 mK at 1.5 K rising to 0.1 K at 100 K,[48] while the temperature *stability* during a field sweep was estimated to vary from about 2 mK at 1.5 K and to about 0.05 K at 100 K.

Magnetic fields parallel to the axis of the measuring coil were produced by a superconducting coil, which gave a maximum field of 25 kOe. The

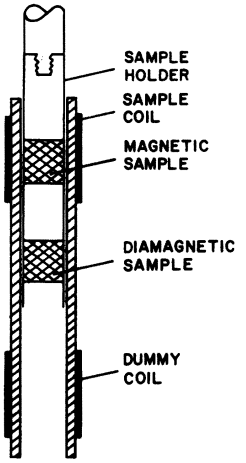

FIG. 4. Details of sample configuration in oscillator coil to reduce dielectric shifts, as explained in text.

inhomogeneity of the field was less than 0.1% over a length of 2 cm, which was quite sufficient for the relatively small samples used in the present experiments. Special care was taken to use a well-regulated power supply, so that it was possible to make measurements without having to activate the persistent-mode switch. This proved to be useful in maintaining a constant temperature for an extended period, and also for speeding the rate at which measurements in different fields could be made.

G. Dielectric Compensation

As mentioned previously, one of the biggest experimental problems was the nonmagnetic ("dielectric") frequency shift Δf_D,[49] which arose from changes in capacitative coupling when the sample was moved relative to the oscillator. To reduce this effect a special design of sample holder was used, and this is shown in Fig. 4. In this arrangement an attempt was made to compensate the capacitative change produced by pulling the magnetic sample out of the coil by replacing it with a dielectrically similar section of sample holder containing a diamagnetic sample. In practice it proved possible in this way to reduce the dielectric shift by a factor of about 10, but for the most accurate measurements it was still necessary to estimate the residual Δf_D experimentally. We shall discuss various ways of doing this in Sec. V B.

Dielectric effects were also minimized in other ways by avoiding the use of unnecessarily high oscillator frequencies (Sec. IV A), and positioning the TDO circuit elements as far as possible from any of the moving parts in the sample transport.

V. ANALYSIS OF EXPERIMENTAL RESULTS

A. General Procedure

In this section we shall go through a step-by-step procedure for processing the raw data in the form of Δf-vs-H measurements to obtain the final result $C_M(0, T)$. To facilitate this discussion we have drawn a schematic flow chart (Fig. 5). It can be seen that there are several points during the course of the analysis at which an evaluation of the best experimental conditions (f, H, and T) becomes possible, and it may become desirable to take additional data which will then permit a simpler analysis. Under the optimum conditions the whole analysis does in fact become quite straightforward and accurate results can be obtained without difficulty. But even in a more general case it is frequently possible to extract very reliable values of C_M, provided care is taken at several crucial steps. In the past these have sometimes been overlooked, and it is our aim to emphasize here some of the complications which may occur.

The first step is to choose appropriate frequency and temperature ranges, and the criteria which govern these have been discussed in some detail in Secs. III A and III B. At the stage of the final analysis it is generally only necessary to verify that the relaxation conditions [Eqs. (3) and (4)] have been satisfied, and this is usually quite evident from the over-all consistency and smoothness of the final results. In particular the breakdown of the spin-lattice relaxation condition shows up as a marked kink in the final C_M results and we shall illustrate this effect in Sec. IV, in which we shall present some of the experimental results which have been obtained.

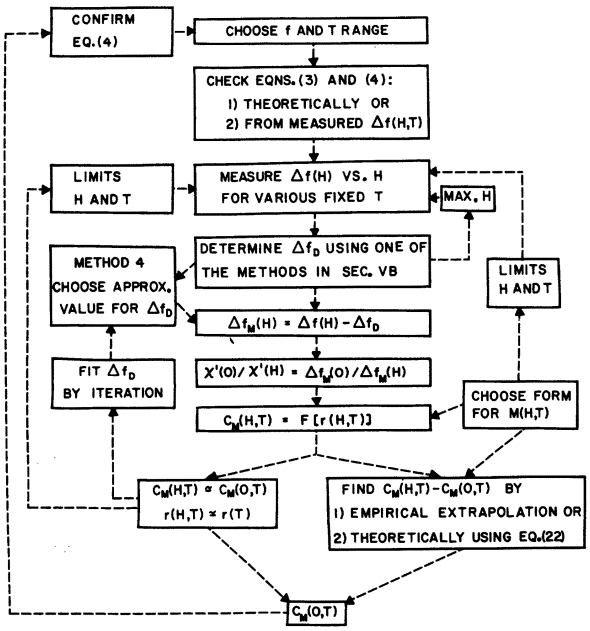

FIG. 5. Flow chart indicating the various steps from measurements of the raw data $\Delta f(H)$ vs H to the final result $C_M(0, T)$. Details are explained in the text.

The next and frequently most difficult step is the determination of the dielectric correction Δf_D. For this there are at least four different procedures, and we shall discuss these in Sec. V B. In three of these one can estimate Δf_D prior to the main analysis, so that one can proceed immediately to estimate Δf_M from the experimentally measured Δf. Unfortunately, none of these three methods is applicable in most of the cases of practical interest, and we generally have to use the fourth method which involves an iterative determination of Δf_D.

Another part of the analysis which generally requires iterative handling is the choice of the maximum dc field, insofar as this is not already limited by the available magnet. As may be seen from the feedback loops indicated in Fig. 5, the maximum H depends on several factors, one of which is the availability of an adequate approximation for $M(H, T)$. We shall discuss this further in Sec. V C and we shall consider some specific approximations in the Appendix. The choice of H also affects the final combination of the different factors in the determination of $C_M(H, T)$ and $C_M(0, T)$, and in Sec. V D we shall discuss the two main cases which can arise. We shall see that the most reliable over-all analysis does not necessarily correspond to the case for which the raw data $\Delta f(H)$ can be determined most accurately; again, a compromise must be made.

As a result of these considerations it is difficult to give a generally valid assessment of the accuracy with which the magnetic specific heat can be measured by the present method, and it is probably most realistic to consider the error estimates in some specific examples. We shall discuss some of these briefly in Sec. VI, where we shall also give references to several publications in which further details of both the analysis and its accuracy can be found.

B. Dielectric Correction

The dielectric shift Δf_D is a small effect (1–100 Hz at 1 MHz), but it is very important since the magnetic shifts are also generally small (~100–5000 Hz). Four methods have been used[21,23] for estimating Δf_D and all are worth considering in specific cases.

(i) In principle it ought to be possible to improve the dielectric compensation to a point where the residual dielectric shift is negligible. This may be practical when the magnetic effects are relatively large, or if some way could be found to cut down the effect of the stray capacity. However, with our present set up and the small samples which we have been using, one of the other methods must be preferred.

(ii) If the temperature dependence of the zero-field susceptibility is known, $\chi'(0, T)$, one can fit measurements of the temperature dependence of the total (zero-field) frequency shift to Eq. (21) to extract Δf_D. This assumes that Δf_D is independent of T, which should certainly be an excellent approximation. The difficulty with this method is that it relies on accurate reproducibility of the sample transport, and as explained in Sec. IV E, this is a difficult problem experimentally. As in the case of the first method, this method may be satisfactory when the magnetic shifts are relatively large or if the appropriate improvement in the apparatus can be made. However, up to now we have been able to use this method only to confirm an independent determination of Δf_D.

(iii) The magnetic contribution to the total Δf decreases with increasing H, and if H can be made large enough ($H \gg H'$), $\Delta f \to \Delta f_D$. This method is excellent provided only that sufficiently large fields are available. It does assume that Δf_D itself is independent of H, which should be a very good approximation inasmuch as Δf_D arises from stray capacities. In general, this method is most suitable for systems with small magnetic specific heats for which sufficiently large fields can be reached relatively easily.

(iv) For most systems it is unfortunately not possible to reach sufficiently large fields to quench Δf_M completely, and an estimate of Δf_D must then be made from a quantitative analysis of the field dependence of $\Delta f(H) = \Delta f_M(H) + \Delta f_D$. Since the field dependence of $\Delta f_M(H)$ is directly related to the determination of $C_M(H, T)$, this amounts to treating Δf_D as an additional parameter to be fitted in the final analysis. We shall therefore defer discussion of this method until Sec. V D, where we shall treat the different cases for determining $C_M(H, T)$.

As in method (iii) we shall assume that Δf_D is independent of H, but in contrast to the method (iii), it will now be very difficult to check this assumption empirically, except insofar as a field dependence of the effective Δf_D might lead to apparent inconsistencies in the over-all analysis. It is therefore more than ever desirable to reduce Δf_D as much as possible, and with this in mind care should be taken to ensure the best dielectric compensation possible in both the design and construction of the apparatus.

Once Δf_D has been estimated we can immediately convert the measured frequency shifts $\Delta f(H)$ to give the desired ratio of susceptibilities:

$$\frac{\chi'(0)}{\chi'(H)} = \frac{\Delta f_M(0)}{\Delta f_M(H)} = \frac{\Delta f(0) - \Delta f_D}{\Delta f(H) - \Delta f_D} \quad . \tag{22}$$

To assess the influence of a small uncertainty $\delta(\Delta f_D)$ in Δf_D on the final C_M, we must consider the effect on $[\chi'(0)/\chi'(H) - 1]^{-1}$ [see Eq. (7), taking $\chi_T(H)/\chi_T(0) \simeq 1$], and using Eq. (22) this gives a

relative error of $\delta(\Delta f_D)/\Delta f_M(H)$. A "typical value"[50] for this may be of the order of 50/5000 = 0.01 and we see that the uncertainty in the dielectric correction can be a major factor in the determination of C_M. This again emphasizes the importance of reducing Δf_D as much as possible and using the best method for estimating its value.

C. Choice of $M(H,T)$

The choice of an appropriate approximation for $M(H, T)$ generally depends on previous knowledge of the system being studied. In the absence of complications from low-lying crystal field levels, the leading term in M can generally be written as a series expansion of the form

$$M = \lambda H \Big/ \left(T + \sum_{n=1}^{\infty} B_n / T^{n-1} \right) , \tag{23}$$

where $-B_1 = \theta$, the usual Curie–Weiss temperature.[51] For $T \gg T_c$, it is customary to neglect all terms beyond B_1, but for the present purpose this introduces an approximation which may be quite significant. This is because a simple Curie–Weiss law satisfies the condtion $(\partial^2 H/\partial T^2)_M = 0$, while a less truncated form does not. From Eq. (12) we see therefore that the higher order terms B_2, $B_3 \ldots$ are essential for understanding the field dependence of $C_M(H, T)$. Conversely of course one can use the observed field dependence at different temperatures to estimate values of B_2, B_3, and in practice this proves to be much more accurate than an analysis of the more usual temperature dependence of M.

However, even with the inclusion of an adequate number of terms B_n, Eq. (23) may still not be adequate for our present purpose. With only terms linear in H, Eq. (23) gives $\chi_T(H)/\chi_T(0) \equiv 1$, and as we discussed in Sec. II A this may be a serious error if $\chi'(0)/\chi'(H)$ is also close to 1. The next order term proportional to H^3 may be written in various approximate forms, of which the simplest is derived from the usual Brillouin function. We shall discuss this and further refinements in the Appendix.

In some cases even the inclusion of a term in H^3 will not be sufficient and higher degree terms may be required. Alternatively, one can always limit the range of H used and this corresponds to one of the feedback conditions indicated in Fig. 5. This becomes particularly relevant at relatively low temperatures where saturation effects might become quite large.

Measurements at low temperatures may be quite important since they allow a comparison between results obtained by the present method with values deduced from calorimetric measurements in a region where the uncertainty due to the lattice contribution is small. Such a comparison can provide a very useful independent check of the parameters used in the linear term [Eq. (23)], and in particular the value of θ which is not determined by the field dependence of C_M.

D. Determination of $C_M(H,T)$

The procedure for determining $C_M(H, T)$ from the measured values of $\Delta f(0)/\Delta f(H)$ depends to a large extent on the appropriate form of the $M(H, T)$ relationship. We can distinguish two main cases, which may be characterized by field dependence of the empirical quantity

$$r(H, T) = H^2/[\chi'(0)/\chi'(H) - 1] \ . \tag{24}$$

In general (case 1) this quantity is a function of both H and T, as indicated by the argument, and to evaluate $C_M(H, T)$ one must substitute measured values of $\chi'(0)/\chi'(H)$ in Eq. (24), using one of the three independent methods to estimate Δf_D. The resulting C_M will generally be field dependent and to extract the desired zero-field specific heat one must find the appropriate extrapolation either theoretically, using Eq. (12), or empirically. We shall discuss the field dependence further in Sec. V E.

A much simpler analysis is possible if $r(H, T)$ is in fact field independent (case 2). This can be ensured by limiting the maximum field, as indicated by the feedback line in Fig. 5. There are two factors which must be satisfied for this case: (a) the field dependence of C_M must be negligible and (b) saturation effects must be small. The latter condition does *not* imply that the saturation terms are necessarily negligible relative to the linear terms, since even in the limit $H \to 0$ the difference of $\chi'(0)/\chi'(H)$ from 1 may be significant. The relative importance of the two factors can readily be established from the form of $M(H, T)$, and in any practical case the limit of $r(H, T)$ as $H \to 0$ can also be found empirically.

In situations where $r(H, T)$ can be predicted to be effectively independent of H, so that $r(H, T) = r(T)$, one can find $r(T)$ from a linear plot of $\chi'(0)/\chi'(H) - 1$ as a function of H^2, and in such a fit it is also easy to include Δf_D as an adjustable parameter. This then is the basis of the fourth and most generally applicable method of estimating the dielectric shift. Great care must be exercised in using this method since any unsuspected field dependence in $r(T)$ can lead to serious systematic errors in Δf_D and the subsequent analysis.

The choice between the two courses of procedure will generally depend on a number of factors and in particular on the accruacy with which small changes in Δf can be detected if only relatively small fields are used. The second case is clearly to be preferred whenever it can be used, since it

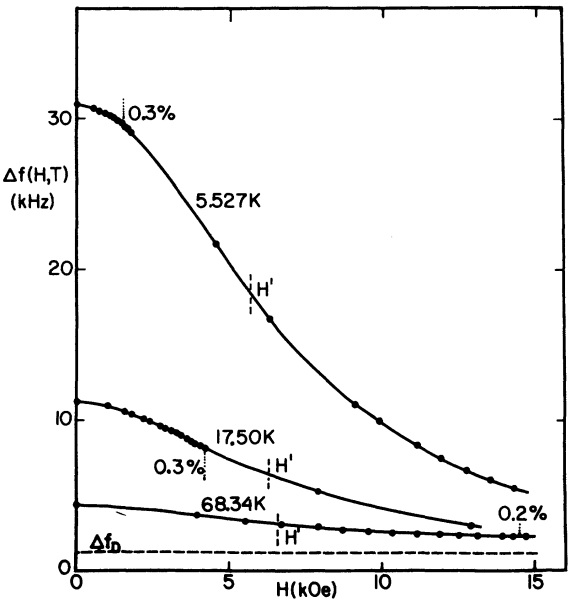

FIG. 6. Field dependence of the total frequency shift $\Delta f(H)$ ($f=4.5$ MHz) for $Gd(OH)_3$ at various temperatures. Fields where 0.2–0.3% field dependence of C_M is expected are indicated. The dielectric shift Δf_D is found from a least squares fit as explained in the text. The three points marked as H' indicate the effective fields estimated from Eq. (15) where Δf_M is roughly reduced to half its zero-field value.

enables $C_M(0, T)$ to be found from measurements at several different fields and a ready check of the consistency is thus possible. However, there is also some advantage in studying the field dependence of C_M, especially at low fields, and we shall discuss this next.

E. Field Dependence of C_M

As explained previously, C_M will be independent of field only under special circumstances, which are generally equivalent to k_BT very much larger than the effect of *either* H or the spin-spin interaction (see Sec. II B). For systems with relatively strong interactions these conditions will usually break down at low temperatures and we must then expect a sizable field dependence.

To analyze this dependence, we note that the leading term will be proportional to H^2 and we write

$$C_M(H, T)T^2/R = C_M(0, T)T^2/R + K_1(T)H^2 + \cdots , \quad (25)$$

where $K_1(T)$ is a function of T which can be calculated from Eq. (12) and the appropriate expression for $M(H, T)$. Equation (25) is, of course, only valid asymptotically, but in most cases higher-order terms will not be very important.

A particularly simple expression for $K_1(T)$ can be obtained when M is adequately represented by Eq. (23), i.e., for low fields. From Eq. (12) we then find that

$$K_1(T) = -(\lambda/R)(B_2 + 3B_3/T + \cdots) \times (T - \theta + B_2/T + B_3/T^2 + \ldots)^{-2} , \quad (26)$$

which, as noted before, is identically zero for the molecular field case $M = \lambda H/(T-\theta)$. It is clear from this expression that a measurement of the field dependence of C_M at low fields and various temperatures can give extremely useful information on the form of the low-field $M(H, T)$ variation.

The general form of Eq. (25) also shows that the appropriate empirical extrapolation to zero field is a plot of $C_M(H, T)$ as a function of H^2, and this has been confirmed by the available results (see Sec. VI).

VI. TYPICAL RESULTS

A summary of all the materials which have been studied with our system so far is given in Table I. Details of the measurements and analysis have been given elsewhere[6,7,23,32–38] and we will here give only a few examples to illustrate the kinds of the results which were obtained.

A. $Gd(OH)_3$

The results for $Gd(OH)_3$ are typical of the class of materials in which orbital effects are negligible and measurements over a wide range of temperatures is possible. Figure 6 illustrates the raw data of $\Delta f(H)$ as a function of H, as obtained from a small (18 mg) crystal at a frequency of about 4.5 MHz. It can be seen that the field required to reduce Δf to half its initial value was about 6 kOe, and since the maximum field available in our system at the time of these measurements was only 15 kOe, the preferred method (iii) for finding Δf_D could not be used. Also since the sample was quite small, the first two methods could not be used with high accuracy. We were therefore forced to use method (iv), fitting Δf_D as part of the complete analysis.

For this it was necessary to establish the field limits over which $r(T, H)$ would be essentially independent of H, and in Fig. 7 we illustrate the observed field dependence of $r(T, H)$ for three widely differing temperatures. In this figure we have already used the finally iterated value of Δf_D to calculate $r(T, H)$; however, a reasonable first estimate of the field dependence could also be obtained from the theoretical $M(H, T)$ relation using low-field susceptibility measurements to estimate θ and B_2. The field ranges over which $r(T, H)$ is constant to better than 0.2 or 0.3% are indicated in Fig. 6, and at each temperature a fit of

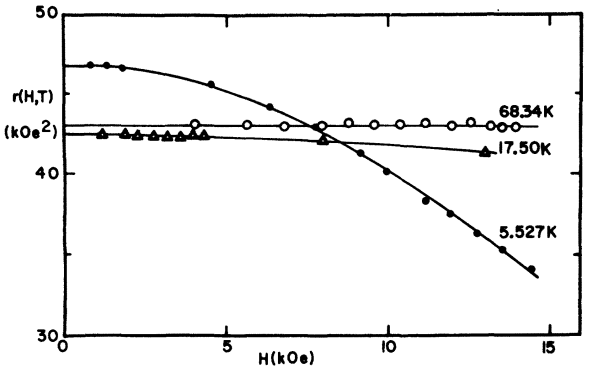

FIG. 7. Field dependence of $r(H, T) = H^2[\chi'(0)/\chi'(H) - 1]$ for $Gd(OH)_3$ for the three fields sweeps in Fig. 6. Only for the highest temperature ($T = 68.34$ K) do we find $r(H, T) = r(T)$ to within 0.2% over the whole field range.

$$(\Delta f(0) - \Delta f_D)/(\Delta f(H) - \Delta f_D) - 1 = H^2/r(T)$$

could be made to find $r(T)$ and Δf_D. No systematic variation of Δf_D was found, and an average over all measurements was therefore used for the final analysis. The corresponding values of $r(T)$ plotted as a function of $1/T$ are shown in Fig. 8.

It can be seen that $r(T)$ is essentially independent of T at high temperatures, as we might expect for a simple system well above its ordering temperature [$T_c = 0.94$ K for $Gd(OH)_3$] (Ref. 6). The corresponding values of $C_M T^2/R$ are shown in Fig. 9, which also includes estimates obtained from calorimetric measurements[6] corrected for the lattice contribution. The agreement between the two sets of data is quite good at the lowest temperatures, confirming the parameters used to describe $M(H, T)$, but at higher temperatures the errors in the calorimetric estimates become so large that a meaningful comparison is impossible.

It is interesting to note the slight curvature of the results when plotted as a function of $1/T$, which indicates that at least three terms in the series expansion [Eq. (1)] are significant at temperatures as high as 5 K in the present case. This corresponds to $T/T_c \simeq 6$, a region in which one frequently assumes that only one term (often denoted by b) might be adequate. Under these conditions it is clearly important to extrapolate $C_M T^2/R$ to find the correct leading coefficients C_2, C_3, etc., and unless measurements can be made over a sufficiently wide temperature range ($T \gg T_c$), this extrapolation may well be in error. With the present method this presents no difficulty, but if we had to rely solely on the calorimetric data the uncertainty would be quite large.

In addition to the low-field measurements it was also possible in this system to study the field dependence of C_M. With the available fields this could be done only at the lowest temperatures and a detailed investigation of the temperature dependence was therefore not attempted, but the effect is clearly illustrated by the results for $T = 5.5$ K shown in Fig. 10. This figure confirms the expected dependence on H^2 at lowest fields, and a comparison between the experimental values and the calculated dotted line also checks the iteratively fitted parameters B_2 and B_3.[6]

B. $Tb(OH)_3$

Generally similar results have been obtained for $Tb(OH)_3$ which, however, differs from $Gd(OH)_3$ in a number of significant features.

First, Tb^{3+} is not an S-state ion and rapid spin-lattice relaxation would be expected at some fairly low temperature which will then limit our method. This temperature was estimated theoretically[7,52] to be about 25 K, and this was clearly confirmed by the final results, which showed a marked kink in the apparent $C_M T^2/R$-vs-$1/T$ curve near 20 K,

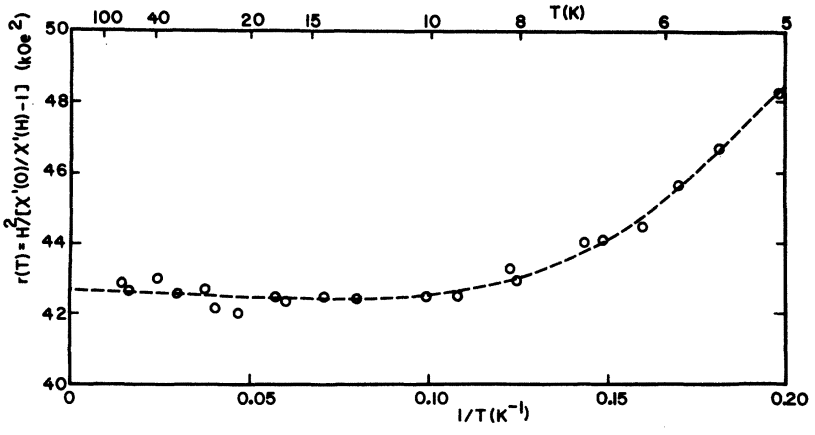

FIG. 8. Temperature dependence of $r(T) = H^2/[\chi'(0)/\chi'(H) - 1]$ for $Gd(OH)_3$ as determined from the relative field dependence of the adiabatic susceptibility. These results are used together with Eq. (A17) to obtain the zero-field magnetic specific heat shown in Fig. 9.

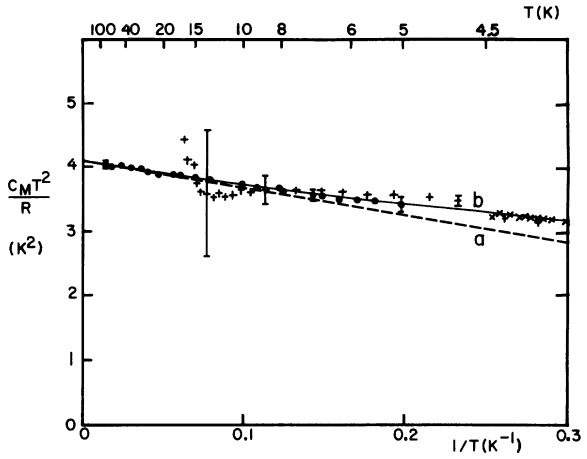

FIG. 9. High-temperature magnetic specific heat for $Gd(OH)_3$ from high-frequency susceptibility measurements (●) and calorimetric measurements (+, ×). There is good agreement between the two sets of data in the region of overlap, but owing to the relative error limits, only the high-frequency data can be used to obtain the correct asymptotic fit [Eq. (1)]. Using an iterative fitting procedure one finds $C_2 = 4.09 \pm 0.05$ K^2 and $C_3 = -4.2 \pm 0.7$ K^3, as indicated by line (a) (Ref. 6). Curve (b) represents a 5-parameter least-squares fit to the data, which indicates that additional high-temperature expansion coefficients $(C_4, \ldots)$ in fact are significant for temperatures as high as $T \sim 5$ K, where $T/T_c \sim 6$.

as indicated in Fig. 11.

The second difference between $Tb(OH)_3$ and $Gd(OH)_3$ is the much higher ordering temperature of $Tb(OH)_3$ ($T_c = 3.72$ K), and we would therefore expect marked deviations from a simple $1/T^2$ law for C_M over most of the accessible temperature range. This is confirmed by the results shown in Fig. 11, and it is evident that care must be taken to extract the correct high-temperature asymptote in this case.

C. Comparison with Calorimetric Data

If one attempted to analyze the usual calorimetric data for $Tb(OH)_3$, which are also shown in Fig. 11, this problem would be even worse since the uncertainties due to the lattice correction completely mask the asymptotic behavior above about 10 K for these measurements. This example illustrates very clearly the advantage of the high frequency relaxation method, but it is perhaps worth repeating that the calorimetric method does offer the very useful possibility of checking the various parameters used in the analysis. Even a relatively small uncertainty in either θ or B_2 can produce a marked change in C_M at the lowest temperatures, and this is demonstrated by the error bars shown in Fig. 11. A comparison between the calorimetric and relaxation data in this region can therefore serve as a sensitive method for refining the values of θ and B_2, or at least checking that realistic error limits have been assigned. The parameters can then be used with confidence at higher temperatures and the principal errors will then be due to uncertainties in measuring the frequency, which can be estimated and improved if necessary.

VII. CONCLUSIONS

In this paper we have reviewed the high-frequency-relaxation (HFR) method for measuring magnetic specific heats. We have shown how recent technical improvements, primarily the developments of tunnel-diode oscillators, frequency counters, and superconducting magnets have extended the range of matrials which can be studied with this method, and we have given a detailed discussion of the conditions which must be satisfied for the method to be applicable.

These conditions may be summarized as follows:

(i) The measuring frequency f must satisfy the two conditions

$$1/\tau_{SL} \ll 2\pi f \ll 1/\tau_{SS} \quad ,$$

where τ_{SL} and τ_{SS} are the spin-lattice and spin-spin relaxation times. This generally sets the upper limit to the temperatures over which measurements can be made.

(ii) To produce a readily measurable effect, a

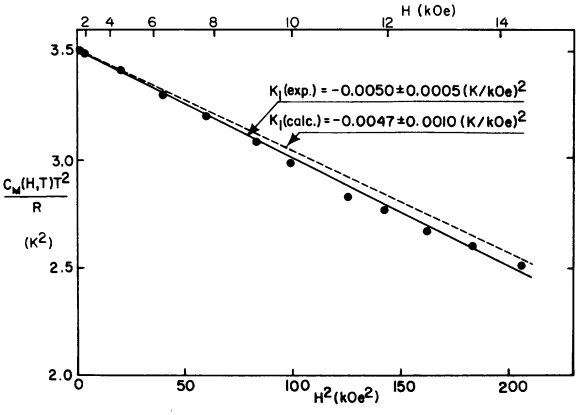

FIG. 10. Field dependence of $C_M(H, T)T^2/R$ for $Gd(OH)_3$ at $T = 5.527$ K as calculated using Eq. (A17) from measurements of $\chi'(0)/\chi'(H)$. The dotted line has a slope $K_1 = -0.0047 \pm 0.0010$ (K/KOe)^2 as determined from theory using the calculated expansion coefficients in the susceptibility ($B_2 = 2.05 \pm 0.10$ K^2, $B_3 = -0.59 \pm 0.10$ K^3) given in Ref. 6. The best fit to the low-field data given $K_1 = -0.0050 \pm 0.0005$ (K/KOe)^2, as shown in the full line in the figure, in excellent agreement with the calculated value. The small discrepancies between calculated and measured values at the highest fields are due to the limited expansions used for both the field and interaction terms, as explained in Ref. 6.

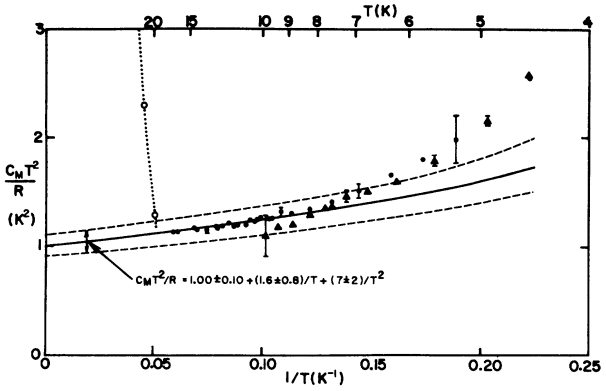

FIG. 11. High-temperature magnetic specific for $Tb(OH)_3$ from measurements of the adiabatic susceptibility (●). At the highest temperatures, a few points are included (○) to illustrate the enormous rise in the apparent measured specific heat when $1/\tau_{SL}$ becomes larger than the oscillator frequency f. This makes it easy to determine experimentally the upper temperature for which condition $2\pi f \gg 1/\tau_{SL}$ is obeyed. Comparison with calorimetric data (▲) shows that the high-frequency data may be expected to give much better values for the leading terms C_2, C_3, and C_4 in the high-temperature expansion [Eq. (1)].

dc field H of the order of

$$H' = (C_M T^2/\lambda)^{1/2}$$

is required, where λ is the Curie constant. With adequate sensitivity considerably smaller fields can sometimes be used.

(iii) An accurate representation of the magnetization must be available for the fields and temperatures used in the experiments.

(iv) If possible, H and T should be adjusted to ranges for which the magnetization satisfies the relation

$$\left(\frac{\partial^2 H}{\partial T^2}\right)_M = 0 \ .$$

The measured specific heat is then independent of H and directly related to the zero-field specific heat calculated theoretically or estimated from more usual calorimetric measurements.

(v) For a simple analysis of the results it is generally also necessary that $T \gg T_c$, so that C_M can be expanded as a series

$$C_M/R = C_2/T^2 + C_3/T^3 + \cdots \ ,$$

where $R = Nk_B$ and N is the number of spins.

(vi) To avoid complicated averages involving the magnetic anisotropy, the material should be either cubic, or available in the form of a single crystal. A fairly simple analysis is also possible if the material is so anisotropic that only one principal component needs be considered in taking the average.

These conditions can be satisfied for a variety of magnetic materials in which the effective spin-spin interactions are not too strong, and so far eight different ionic rare-earth insulators with ordering temperatures between 0.1 and 4 K have been studied with our system. Extension to other kinds of materials with ordering temperatures up to 10 or 20 K seems quite practical, and in some cases materials with even stronger interactions may be suitable. Owing to the high-frequency nature of the method it is difficult to envisage its application to metallic systems, except perhaps for some powders of cubic materials.

Another possible extension of the method is to systems close to or below their ordering temperatures. This would present a number of problems in both the experimental technique and the analysis, but if these could be overcome, a very much larger class of materials could be studied by this method.

Even in absence of such major innovations there are a number of technical improvements which could probably extend the usefulness and accuracy of the method, and several of these are now undergoing preliminary tests. These include improvements in the sample transport mechanism, attempts to reduce the dielectric shift, changes in the dc bias leads to reduce temperature sensitivity of the oscillator, and the use of several readily interchangeable oscillators to facilitate the comparison of measurements at different frequencies. It would also be advantageous to standardize the oscillator rf coil and sample holder design so that comparisons between different experimental results could be made more readily.

But even without these improvements, it seems fairly clear that the HFR method based on the kinds of techniques which we have described here is already a very useful addition to the experimental tools for studying magnetic materials, and certainly one which warrants further development.

ACKNOWLEDGMENTS

We would like to thank R. B. Clover for a number of valuable discussions about his original high frequency system and for help with some of the early experiments. We would also like to acknowledge the expert assistance of C. Sneider in the construction of the apparatus and the valuable contributions of S. Mroczkowski, H. E. Meissner, and J. Eckert in growing the crystals used for the experiments. One of us (W. P. W.) would also like to thank the Physics Department of the Brookhaven National Laboratory for their gracious hospitality during the preparation of this manuscript.

APPENDIX

In this Appendix we shall consider a few simple approximations for $M(H, T)$ which may be adequate

at high temperatures ($T \gg T_c$) and low fields (Zeeman energy $\ll k_B T$), in systems for which there are no complications from crystal field effects. In each case we shall give expressions for $C_M(H, T)$ and $C_M(0, T)$ in terms of the experimentally determined ratio $\chi'(0)/\chi'(H)$, corresponding to the general expressions Eqs. (7) and (12).

Case A

For a simple Curie–Weiss law

$$M = \lambda H/(T-\theta) \tag{A1}$$

we find

$$\frac{C_M(0, T)T^2}{R} = \frac{C_M(H, T)T^2}{R} = \frac{\lambda}{R}\left(\frac{T}{T-\theta}\right)^3 r(H, T) \ , \tag{A2}$$

where

$$r(H, T) = H^2/[\chi'(0)/\chi'(H) - 1] \ . \tag{A3}$$

It is evident from Eq. (A2) that $r(H, T)$ is independent of H in this case, and in general this is the only case for which $C_M(H, T)$ itself is not field dependent.

Case B

A more accurate low-field expression can be written in the form

$$M = \lambda H \Big/ \left(T + \sum_{n=1}^{\infty} B_n/T^{n-1}\right) \ , \tag{A4}$$

where $-B_1 = \theta$, as mentioned previously. This leads to

$$\frac{C_M(H, T)T^2}{R} = \frac{\lambda}{R}\left(\frac{T}{T-y}\right)^3 (1-y')^2 r(H, T) \tag{A5}$$

and

$$\frac{C_M(0, T)T^2}{R} = \frac{C_M(H, T)T^2}{R} - \frac{1}{2}\frac{\lambda}{R} y'' T^3 \frac{H^2}{(T-y)^2} \ , \tag{A6}$$

where

$$y = -\sum_{n=1}^{\infty} B_n/T^{n-1} \ , \tag{A7}$$

$$y' = \frac{dy}{dT} = \sum_{n=2}^{\infty} (n-1)B_n/T^n \ , \tag{A8}$$

$$y'' = \frac{dy^2}{dT^2} = -\sum_{n=2}^{\infty} n(n-1)B_n/T^{n+1} \ . \tag{A9}$$

Case C

To take account of large fields one can start with the usual Brillouin function

$$M = B_{S'}(g\mu_B H/k_B T) \tag{A10}$$

and one can include the effect of spin-spin interactions to first order by replacing H by

$$H_{eff} = H + pM \ , \tag{A11}$$

where p is related to the previous representation of the interactions by $p = \theta/\lambda$. For arbitrary H one must solve Eqs. (A10) and (A11) iteratively, but to order H^3 one can obtain a closed expression for M:

$$M = \frac{\lambda H}{T-\theta}\left(1 - \frac{1}{3}\alpha_{S'} H^2 \frac{T}{(T-\theta)^3}\right) \ , \tag{A12}$$

where

$$\alpha_{S'} = \tfrac{1}{10}(g\mu_B/k_B)^2[2S'(S'+1)+1] \ . \tag{A13}$$

Substituting this in Eq. (7) one gets

$$\frac{C_M(H, T)T^2}{R} \simeq \frac{\lambda}{R}\left(\frac{T}{T-\theta}\right)^3 r(H, T) \times \left(1 + \alpha_{S'} r(H, T)\frac{T}{(T-\theta)^3}\right) \ , \tag{A14}$$

where we have assumed $\alpha_{S'}[T/(T-\theta)^3]H^2 \ll 1$ and $\theta/T \ll 1$. Using Eq. (12) we also get

$$C_M(0, T)T^2/R \simeq C_M(H, T)T^2/R \ . \tag{A15}$$

In principle, one could extend these expressions to higher powers in H, but in practice it is generally more important to consider higher orders of the interaction effects.

The last term in Eq. (A14) shows that the effect of magnetic saturation can be important even for small H, depending only on the relative size of $\alpha_{S'}$, $r(H, T)$, T, and θ.

Case D

The simultaneous inclusion of higher order interaction and Zeeman terms is quite difficult and requires information about the specific form of the interaction Hamiltonian. The general methods are well known[3,53] and specific applications to simple Ising systems have been given elsewhere.[7,35]

Here we shall only consider a phenomenological approximation which combines the correct treatment of the interactions in the term linear in H, as in Eq. (A4), with the mean-field approximation for the term in H^3 as given in Eq. (A12). We therefore write

$$M \simeq \frac{\lambda H}{T-y} - \tfrac{1}{3}\lambda\alpha_{S'} H^3 \frac{T}{(T-\theta)^4} \ . \tag{A16}$$

This expression must be used with care since the two terms are correct to quite different orders in the interactions, but if H is kept small, Eq. (A16) can in fact provide a very useful improvement over the linear approximation of Eq. (A4).

Using Eq. (7), we now obtain

$$\frac{C_M(H, T)T^2}{R} \simeq \frac{\lambda}{R}\left(\frac{T}{T-y}\right)^3 (1-y')^2 r(H, T)$$

$$\times\left(1+\alpha_S\cdot r(H,T)\,\frac{T}{(T-\theta)^3}\right), \qquad \text{(A17)}$$

where we have made the same approximations as for Eq. (A14). Using Eq. (12) we also get

$$\frac{C_M(0,T)T^2}{R} \simeq \frac{C_M(H,T)T^2}{R} - \frac{1}{2}\,\frac{\lambda}{R}\,y''T^3\,\frac{H^2}{(T-y)^2}\,. \qquad \text{(A18)}$$

Although these expressions are clearly limited in their accuracy, they have been found to be adequate for a wide variety of materials (see Table I), provided only that care is taken not to exceed the appropriate maximum field or to go too close to the ordering temperature. As a general rule the corrections introduced by the paramagnetic saturation terms may be quite erroneous whenever higher than first order interaction terms cannot be neglected, i.e., for temperatures where $B_2/T \sim \theta$.

---

*Supported in part by the National Science Foundation.

[1]We use the symbol C_M to denote in particular the magnetic specific heat at constant magnetization. As we shall see in Sec. II this is equal to the specific heat in zero external field in many cases, and in other cases the two can be related by a simple thermodynamic formula.

[2]W. Opechowski, Physica (Utr.) **4**, 181 (1937).

[3]J. H. Van Vleck, J. Chem. Phys. **5**, 320 (1937).

[4]J. M. Daniels, Proc. Phys. Soc. Lond. **66**, 673 (1953).

[5]We have here followed the usual practice of expressing C_M in units of $R = Nk_B$, where N is the number of spins and k_B is Boltzmann's constant. If N is Avogadro's number, $R = 8.31$ J/mole K. The coefficients C_n then have the dimension of (K^n).

[6]A. T. Skjeltorp, C. A. Catanese, H. E. Meissner, and W. P. Wolf, Phys. Rev. B **7**, 2062 (1973).

[7]C. A. Catanese, A. T. Skjeltorp, H. E. Meissner, and W. P. Wolf (unpublished).

[8]H. B. G. Casimir and F. K. du Pré, Physica (Utr.) **5**, 507 (1938).

[9]C. J. Gorter, *Paramagnetic Relaxation* (Elsevier, New York, 1947).

[10]A. H. Cooke, Rep. Prog. Phys. **13**, 276 (1950).

[11]C. J. Gorter, Prog. Low Temp. Phys. **II**, 267 (1957).

[12]C. J. Gorter, in *Fluctuation, Relaxation and Resonance in Magnetic Systems*, edited by D. ter Haar (Plenum, New York, 1962), p. 87.

[13]In addition many papers in Physica (Utr.) and Communications from the Kammerlingh Onnes Laboratory.

[14]K. W. Mess, J. Lubbers, L. Niesen, and W. J. Huiskamp, Physica (Utr.) **41**, 260 (1969).

[15]B. M. Abraham, O. Brandt, Y. Eckstein, J. B. Ketterson, M. Kuchnir, and P. Roach, Phys. Rev. **187**, 273 (1969).

[16]O. W. G. Heybey, thesis (Cornell University, 1962) (unpublished).

[17]C. Boghosian, H. Meyer, and J. E. Rives, Phys. Rev. **146**, 110 (1966).

[18]J. F. Jarvis, D. Ramm, and H. Meyer, Phys. Rev. **170**, 320 (1968).

[19]P. R. Critchlow, R. A. Hemstreet, and C. T. Neppell, Rev. Sci. Instrum. **40**, 1381 (1969).

[20]R. T. Harley, J. C. Gustafson, and C. T. Walker, Cryogenics **10**, 510 (1970).

[21]R. B. Clover and W. P. Wolf, Rev. Sci. Instrum. **41**, 617 (1970).

[22]F. Rothwarf, D. Ford, and L. W. Dubeck, Rev. Sci. Instrum. **43**, 317 (1972).

[23]R. B. Clover and W. P. Wolf, Solid State Commun. **6**, 331 (1968).

[24]The original Casimir–du Pré theory was based on a classical description of the spins and lattice viewed as independent thermodynamic systems each in internal equilibrium. A more general quantum-mechanical discussion of this type of problem has been given more recently by H. Schwegler and G. Sauermann [Z. Phys. **204**, 375 (1967); Z. Phys. **209**, 355 (1968)], but under the simplifying conditions corresponding to the present method, the results are the same as for the classical description.

[25]R. Orbach, Proc. R. Soc. A **264**, 458 (1961); Proc. R. Soc. A **264**, 485 (1961).

[26]J. C. Verstelle and D. A. Curtis, in *Handbuck der Physik*, edited by H. P. J. Wijn (Springer-Verlag, Berlin, 1968), Vol. 18, part 1, p. 1.

[27]W. J. Caspers, *Theory of Spin Relaxation* (Interscience, New York, 1964).

[28]G. Sauermann, Physica (Utr.) **32**, 2017 (1966).

[29]I. Nowik and H. H. Wickman, Phys. Rev. **140**, A869 (1965).

[30]There may be complications if crystal-field effects are larger than the spin-spin interactions, and in this case the simple asymptotic form will not be reached until $k_BT \gg V_c$, where V_c represents the size of the crystal-field effects.

[31]The Curie constant λ must here be taken in units corresponding to those of C_M, e.g., g atom of the magnetic spins in question.

[32]R. B. Clover, thesis (Yale University, 1969) (unpublished).

[33]R. B. Clover and R. J. Birgeneau, J. Appl. Phys. **40**, 1151 (1969).

[34]A. T. Skjeltorp and W. P. Wolf, J. Appl. Phys. **42**, 1487 (1971).

[35]A. T. Skjeltorp and W. P. Wolf, AIP Conf. Proc. **5**, 695 (1972).

[36]E. Becker and R. B. Clover, Phys. Rev. Lett. **21**, 1327 (1968).

[37]R. B. Clover (unpublished).

[38]R. B. Clover and A. T. Skjeltorp, Physica (Utr.) **53**, 132 (1971).

[39]For the present we shall neglect here possible complications due to anisotropy effects (see Sec. III E).

[40]An improved version of a tunnel-diode oscillator has recently been built and tested by C. T. Van Degrift at University of California, Irvine. [Presented at the Thirteenth International Conference on Low Temperature Physics in Boulder, Colo., 1972 (unpublished).]

[41]In some cases it may be either undisirable or impossible to reach such large values of $\Delta f_M(0)/\Delta f_M(H)$ (see Secs. V C and V D). For the present discussion we also assume that $\Delta f_M \gg \Delta f_D$.

[42]F. J. Kopp and T. Ashworth, Rev. Sci. Instrum. **43**, 327 (1972).

[43]T. M. Dauphineé and H. Preston-Thomas, Rev. Sci. Instrum. **25**, 884 (1954).

[44]H. S. Sommers, Rev. Sci. Instrum. **25**, 793 (1954).

[45]The insensitivity to fields was due to both a relatively low intrinsic magnetoresistance and the fact that the sensors were positioned outside the bore of the magnet.

[46]CryoResistor, type CR 2500H, CryoCal Inc., Fla.

[47]According to specifications supplied by the manufacturer (Ref. 46).

[48]From figures furnished by the manufacturer (Ref. 46).

[49]The "dielectric" shift Δf_D also includes contributions from the temperature-independent paramagnetic (Van Vleck) and diamagnetic susceptibilities. These are generally quite small and with the present experimental arrangement they account for

only a small fraction of the observed Δf_D. Their effect might become more important in a more refined system in which the stray capacities could somehow be reduced.

[50]This value applies specifically to the example of $Gd(OH)_3$ at 4.5 MHz and 17 K, in a field $H = 7\text{kOe} \approx H'$. At higher temperatures, fields, or frequencies the relative effect of the dielectric correction would be larger and vice versa.

[51]We ignore here the temperature-independent paramagnetic and diamagnetic contributions whose effect may be absorbed into Δf_D (see Ref. 49).

[52]A. T. Skjeltorp, thesis (Yale University, 1971) (unpublished).

[53]J. S. Smart, *Effective Field Theories of Ferromagnetism and Antiferromagnetism* (Saunders, Philadelphia, Pa., 1965).

PHYSICAL REVIEW B VOLUME 8, NUMBER 1 1 JULY 1973

Magnetomechanical Ratios and Spin and Orbital Moments for Ni-Cu Alloys

G. G. Scott and R. A. Reck
Research Laboratories, General Motors Corporation, Warren, Michigan 48090
(Received 21 November 1972)

Magnetomechanical ratios (g') have been measured for eight different Ni-Cu alloys in the range 0–30.68-at.% copper. Values of g' decrease linearly with increasing Cu composition to about 24-at.% Cu and then drop off more rapidly. The results have been combined with saturation magnetization measurements from the literature to obtain values of the orbital and the spin contribution to the average moments. Based upon a short-range-order magnetic model the local electronic orbital moment is found to be $\sim 0.05\ \mu_B$ for all combinations of nearest and second-nearest neighbors.

I. INTRODUCTION

We have previously measured magnetomechanical ratios[1] for the binary alloys of Fe, Co, and Ni. This previous work has shown that the g' value for a particular binary alloy cannot be predicted by an analysis which considers the g' values of the constituent atoms to be the same as those measured for the pure metals.

Recently, ferromagnetic-resonance experiments have been conducted on a group of Ni-Cu alloys.[2] These experiments indicated that all of these alloys have the same g factor (2.19 ± 0.03) as that for pure nickel. This g-factor constancy is contrary to our g' findings where simple additivity for binary alloys is not sufficient to determine effective g' values.

The Ni-Cu alloy system forms a continuous series of solid solutions and all of the alloys have the face-centered-cubic-structure characteristic of pure Cu or pure Ni. In addition, this alloy system has long been considered as the prototype for a simple rigid-band model. Because of both the structural and assumed theoretical simplicity, many investigations of the magnetic properties of these alloys have appeared in the literature. It was therefore thought that it would be of value to extend our g' investigations to include alloys of this system.

The present investigation has shown that g' values are steadily reduced with an increase in dissolved copper. These g' changes, however, are small and would have been unobserved in the resonance experiments in Ref. 2.

II. EXPERIMENTAL

Our method of measuring g' by means of the Einstein–de Haas effect has been previously described.[3] Using these techniques we have determined room-temperature g' values for pure nickel and for eight different Ni-Cu alloys in the range 0–30.68-at.% Cu. Higher copper concentrations could not be used, since cooling was not available to reduce the temperature below the Curie points of these alloys.

The samples used were cylinders 1.5 cm in diameter and 32 cm long. These cylinders were accurately ground so as to fit into a magnetizing winding which formed an integral part of a delicate torsional pendulum. The experimental technique involves measuring the angular acceleration induced by reversing the magnetization of the sample. Nickel, of course, has an unusually large magnetostrictive coefficient. Although magnetostrictive forces are independent of the magnetization direction, it is possible to obtain stress changes upon reversal if any permanent sample magnetization exists. Our samples were therefore annealed for 4 h, in an inert atmosphere at 750 °C in order to remove both internal stress and permanent magnetization, and hence to eliminate the possibility of obtaining extraneous pendulum accelerations. A semiquantitative spectroscopic analysis was also made for these samples. This analysis indicated the major impurities to be Si and Fe which were present, at most, to a few tenths of 1%.

The results of the g' experiments are given in Table I, where the error range is the average de-